Prediction of Cutting Temperature Distribution in Transient Heat Conduction of Monolayer Coated Tools Based on Non-Fourier Heat Conduction during Machining of H13 Hard Steel

Ipilakyaa Tertsegha Daniel[1*], Bam Sebastine Aondover[2], Tuleun Livinus Tyovenda[3]

Department of Mechanical Engineering, Joseph Sarwuan Tarka University, Makurdi, Benue State-Nigeria
*Corresponding Author

Received: 04 August 2023/ Revised: 17 August 2023/ Accepted: 23 August 2023/ Published: 31-08-2023

Abstract— *A predictive model for transient heat conduction during the machining of hard steel based on non-Fourier heat conduction was developed. A mono layer cutting tool coated with TiN coating of carbide substrate was used with 2μm thickness. The work piece material used was a cylindrical bar of H13 hard steel, 300mm length and 70mm external diameter. The cutting speed range was 35.9-244.4m/min, feed rate of 0.2m/rev and depth of cut of 0.2mm. A developed wireless temperature measurement was employed with the thermocouple sensor embedded in the turning tool. The developed model is simplified and contains hypothetical conditions. An infinitesimal convective heat conduction coefficient makes the boundary to be an adiabatic or thermostatic boundary. During machining, the coated tool and workpiece material's heat dissipation are neglected. Prediction was done and compared between the Fourier heat conduction model and the non-Fourier heat conduction to reveal the non-Fourier model effect on transient heat conduction. Predictions by the two models are considerably dissimilar with 77.10C difference at 0.1s cutting time. The predicted temperature difference between the two models when the cutting duration is 10 s is 4.90C. The temperature tends to stabilize when the cutting time is sufficient and heat conduction reaches its steady state. From the results, it can be concluded that the transient heat conduction model is more suitable for the intensity transient-state in the process of cutting heat conduction. The prediction error is less than 12%, which is acceptable for industrial applications and proves the efficiency of the developed model.*

Keywords— Cutting Temperature, Coated Tool, Laplace Transform, Non-Fourier Heat Conduction, Transient Heat Conduction.

I. INTRODUCTION

In recent years, more and more coated tools have been used in metal cutting operations, particularly when machining materials that are challenging to machine. The hardness and wear resistance of the tool are both increased by the application of a tool coating [1,2]. The thin film coating on the cutting tool surface contributes significantly to the process of heat conduction into the cutting tool body and can increase tool strength and reduce friction between tools and workpieces. For the investigation of the thermal effect on tool life and workpiece quality, the analysis of the temperature distribution within the tool's body is crucial. During the cutting process, coated tools generate and conduct heat considerably different from uncoated tools due to the presence of the tool coating film. The tool coating's low coefficients of friction can minimize the cutting force and temperature. The tool coating can also be used as a heat-resistant material for cutting tools to stop excessive temperature from escaping into the tool matrix. Because of this, coated tools are frequently used in machining [3], and the coating clearly increases a tool's lifespan.

Three states of heat conduction can be distinguished during the cutting process: the intensity transient state, the transient state, and the steady state. The cutting temperature in steady-state heat conduction was extensively studied using Fourier heat conduction. To explain the change in coated tool temperature during dry milling of nickel-based super alloys for a turbine blade, Sijie Yan et al. [4] proposed a thermal model. The model was developed using steady-state heat conduction differential equations. To estimate the tool temperature distribution at various tool states, the proposed model calculates both the heat fluxes into the tool from the rake face and due to flank wear. The affect of flank wear is viewed according to the rapid tool wear mechanism. The impact of coating materials on the thermal behavior of a body exposed to numerous moving heat sources

was investigated by Bari et al. [5]. They determined steady-state temperature using the finite complex Fourier transform and the finite cosine Fourier transform. A novel method to assess the cutting temperature for the milling process was presented by Benabid et al. [6]. The FEM's numerically and experimentally determined temperatures at the same boundary condition were then compared to the predicted temperature from the previously presented analytical model. The results of the comparisons revealed that there is good agreement between the temperatures obtained from experimental measurement, FEM simulation, and analytical prediction.

The Fourier heat conduction in steady-state heat conduction provides a good description of the evolution of the cutting temperature. To do the numerical computation, however, various safety measures are required when heat conduction is quick and transient [7,8]. Heat conduction is defined as heat propagating at a finite speed in transient heat conduction of rapid heat flow, when the time of thermal action is frequently less than the material's thermal relaxation time. The other points in the heat-conducting medium will be simultaneously impacted by the thermal disturbance when some points in the heat-conducting medium exhibit thermal disturbance. Since light travels at a constant speed, it is physically impossible for heat to move at a faster rate. The idea that the thermal disturbance velocity is infinite is unacceptable. The temperature fluctuates quickly for the unsteady-state of the heat conduction process, including high (or low) temperature circumstances, a super high velocity of heat conduction, and under micro space or a very short time scale of heat conduction. The unsteady-state heat conduction has not been suitable for the Fourier assumption of heat conduction, which assumes the heat conduction velocity is infinite. By introducing the Caputo-type fractional Cattaneo sub diffusion model to investigate the anomalous diffusion process in the temperature response of the two-phase system, Mozafarifard et al. [9] intend to perform the quick-transient heat-flow method in a porous material. Due to the assumption that the thermal wave propagates at an infinite rate and that thermal interactions between phases take place concurrently, the conventional Fourier model is unable to explain such effects. The most precise forecast of the transient process of heat flow in a solid-fluid system under the brief thermal perturbation is provided by the fractional time differentiation term, which may interpret the memory effects of the physical problem. Zehnder [10] used infrared temperature measurement to track the thermal wave phenomenon in AISI4340 carbon steel. According to the experimental findings, the region of intensive heating would not be able to use the conventional Fourier heat conduction due to the large temperature increases over ambient. In the cutting intensity transient-state, it is important to consider the non-Fourier heat conduction in micro or nanopascal heat conduction for metal materials modified by the traditional Fourier heat conduction.

The non-Fourier heat conduction was independently proposed in the 1960s by Cattaneo [11] and Vernotte [12]. Hyperbolic partial differential equations are its mathematical representation. The features of non-Fourier heat conduction effects, such as a very short duration of a thermal effect, thermal heating material on a small or medium scale, or fully departing from the traditional Fourier heat conduction effect, were specified for the abnormal condition Fourier heat conduction effect. Many scholars have attempted to solve the hyperbolic heat conduction equation under various physical circumstances, developing a number of mathematical techniques to precisely predict various physical geometries and boundary conditions for the temperature field [13,14]. By using the one-dimensional liquid bath's solidification kinetics, Schwarzwlde et al. [15] investigated non-classical heat transfer in phase-change processes as modeled by the Maxwell-Cattaneo (MC) and Guyer-Krumhansl (GK) equations.

With varying degrees of success, many methods have been put forth to model the temperature at which coated tools cut metal. In addition to complex experimental methods, a number of analytical and numerical approaches have been suggested to describe the temperature distribution. The effect of coatings on a cutting tool was numerically analyzed by Ferreira et al. [16]. The coating did an excellent job of shielding the cutting tool's substrate from heat. Zhang et al.'s [17] analysis of coating materials' effects on transient heat conduction revealed that the coating possesses a thermal barrier feature that prevents heat transmission during machining. In this study, a novel method based on non-Fourier heat conduction is presented for forecasting the cutting temperature distribution in transient heat conduction of monolayer coated tools. To demonstrate the existence of the non-Fourier heat conduction effect in the transient state, the features for temperature distribution in unsteady-state and steady-state are compared and analysed. The temperature distribution of a TiN-coated instrument during transient heat conduction allows us to see the fluctuating change process of the temperatures.

II. MODELLING OF HEAT CONDUCTION IN COATED TOOLS

Figure 1 [18] illustrates how heat is produced during the cutting process at the shear plane by main deformation, the tool-chip contact, and the tool-workpiece interface through friction. The area next to the cutting edge receives most of the heat produced. Due to the three heat sources' extremely proximity to one another and the speed of the cutting process, it is challenging to

measure or calculate the amount of heat flux on the rake face. For the sake of simplicity, it is assumed that there is no temperature gradient in the rake face and that the tool body contains neither a heat source nor a heat generator. As indicated in Figure 1, the generated heat can be interpreted as one equivalent constant temperature acting in one-dimensional heat conduction on the coated tool's rake face.

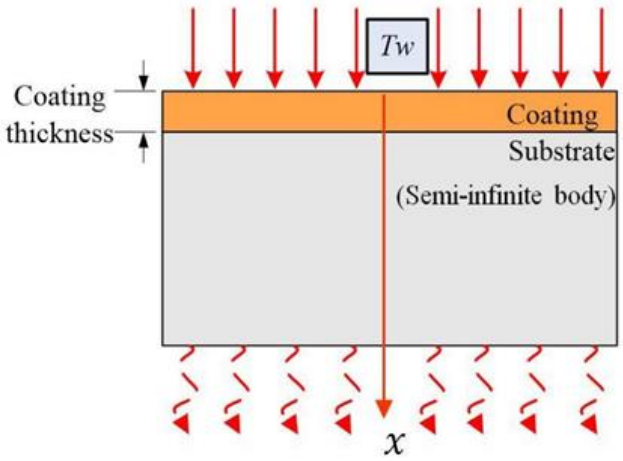

FIGURE 1: Heat source and the equivalent heating temperature of the cutting tool.

The typical coating thickness for monolayer coated tools is between 1 to 8 m [19]. The tool coating experiences a powerful immediate thermal shock when it penetrates the work piece. The transient degree steadily decreases as cutting time increases and eventually transitions to steady-state heat conduction. The coated tool substrate can be thought of as a semi-infinite body because it is sufficiently huge when compared to a mono-layer coating. A one-dimensional coated tool's schematic heat conduction model is shown in Figure 2. These presumptions were utilized in the heat conduction calculation:

1. Machining is done at ambient temperature under the assumption that the initial temperature of the tool and the workpiece is the same ($T_0 = 20^0C$).
2. The thin coating layer and the tool substrate will allow the heat flux into the coated tools to pass through without being lost in any other way. There is no heat transfer to the surroundings.

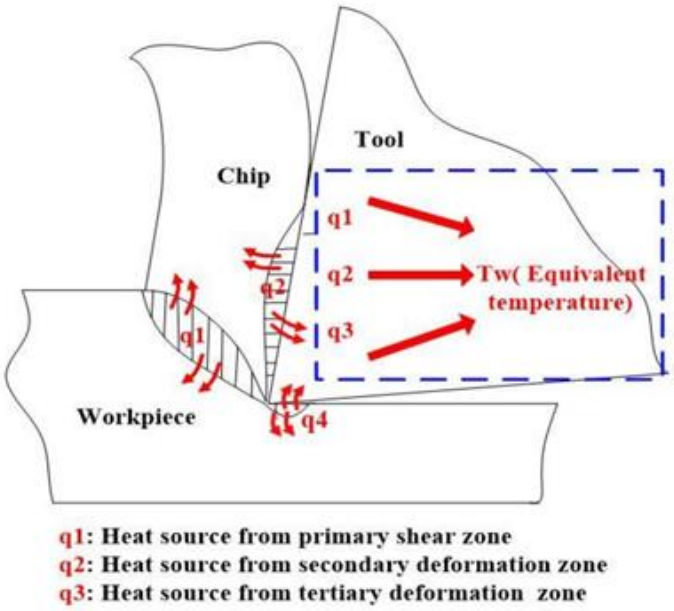

FIGURE 2: Schematic diagram of a one-dimensional heat conduction model of coated tools.

The following assumptions are made for the purpose of obtaining the mathematical modelling of the proposed unsteady-state heat conduction process.

1. For a coating layer, thermal properties like conductivity and diffusivity are homogeneous and independent of temperature.

2. As depicted in Figure 2, the cutting tool's substrate body is a semi-infinite body along the coating thickness direction.

The non-Fourier law of heat conduction is used to create the unsteady-state heat conduction model of the mono-layer coated tool based on the established one-dimensional heat conduction model of the coated tools. The cutting heat conduction direction is in the x-axis. The transient temperature at point (x, t) is represented by the continuous function T (x, t), where x and t are the space and time coordinates respectively. In the course of cutting, it is assumed that the ambient temperature is T0. The rake face of the coated tool is shocked by an analogous constant temperature Tw (Tw > T0) when the cutting time is t = 0+. Tw is considered to always act on the coating's top surface and to be constant during the process of heat conduction. The thermal diffusivity of the coating material (a), the relaxation time (τ) , the heat flux (q), the coating thickness (d), and the thickness of the coated tool (L) are all given. In light of the aforementioned, it is presumable that heat only travels in the direction of coating thickness. The following is the mathematical model that uses non-Fourier heat conduction to describe the temperature field of T (x, t) in the coating:

$$a\frac{\partial^2 T}{\partial x^2} = \tau_0 \frac{\partial^2 T}{\partial t^2} + \frac{\partial T}{\partial t}\ 0 < x < d, t \geq 0 \tag{1}$$

Initial conditions:

$$\begin{aligned} &T(x,t)|_{t=0} = T_0\ 0 \leq x \leq d \\ &\left.\frac{\partial T(x,t)}{\partial t}\right|_{t=0}\ 0 \leq x \leq d \end{aligned} \tag{2}$$

Boundary conditions:

$$\begin{aligned} &T(x,t)|_{x=0} = T_w\ t \geq 0 \\ &\left.\frac{\partial T(x,t)}{\partial t}\right|_{x=t}\ t \geq 0 \end{aligned} \tag{3}$$

The illustration of the initial conditions is the temperature of the cutting tool remains at T_0 before heat load effects at the boundary, and it is in a natural state. The boundary condition is that the coated tool is an adiabatic boundary during heat conduction.

To introduce the excess temperature T*,

$$T^*(x,t) - T_0 \tag{4}$$

Then, the heat conduction control equation, initial conditions, and boundary conditions become the following:

Heat conduction control equations:

$$a\frac{\partial^2 T^*}{\partial x^2} = \tau_0 \frac{\partial^2 T^*}{\partial t^2} + \frac{\partial T^*}{\partial t}\ 0 < x < d, t \geq 0 \tag{5}$$

Initial conditions:

$$\begin{aligned} &T^*(x,t)|_{t=0} = 0\ 0 \leq x \leq d \\ &\left.\frac{\partial T^*(x,t)}{\partial t}\right|_{t=0}\ 0 \leq x \leq d \end{aligned} \tag{6}$$

Boundary conditions:

$$\begin{aligned} &T^*(x,t)|_{x=0} = T_w\ t > 0 \\ &\left.\frac{\partial T^*(x,t)}{\partial t}\right|_{x=t} = 0\ t > 0 \end{aligned} \tag{7}$$

Equation (5) is conducted to a Laplace transform:

$$\overline{T}^*(x,s) = L[T^*(x,s)] = \int_x^\infty T^*(x,t)e^{-st}dt \tag{8}$$

$$a\frac{\partial^2 \overline{T}^*}{\partial x^2}(x,s) = s\overline{T}^*(x,s) - T^*(x,0) + \tau\left[s^2\overline{T}^*(x,s) - sT^*(x,0) - \frac{\partial}{\partial t}T^*(x,0)\right] \tag{9}$$

The initial conditions (6) into Equation (9) are as follows:

$$a\frac{\partial^2\overline{T}^*}{\partial x^2}(x,s) = (s+\tau s^2)\overline{T}^*(x,s) \tag{10}$$

The solution of Equation (10) is as follows:

$$\overline{T}^*(x,s) = A(s)e^{-\sqrt{\frac{s+\tau s^2}{a}}x} + B(s)e^{\sqrt{\frac{s+\tau s^2}{a}}x} \tag{11}$$

The boundary conditions (7) are obtained by Laplace transform:

$$\begin{aligned} &\overline{T}^*(x,s)\Big|_{x=0} = \frac{T_w - T_0}{s} \\ &\frac{\partial\overline{T}^*(x,t)}{\partial t}\Big|_{x=d} = 0 \end{aligned} \tag{12}$$

Substituting Equation (12) into Equation (11) gives the following:

$$A(s) + B(s) = \frac{T_w - T_0}{s} \tag{13}$$

$$A(s)e^{-\sqrt{\frac{s+\tau s^2}{a}}x} + B(s)e^{\sqrt{\frac{s+\tau s^2}{a}}x} = 0 \tag{14}$$

From Equations (13) and (14),

$$A(s) = \frac{T_w - T_0}{s} \times \frac{1}{1-e^{-2\sqrt{\frac{s+\tau s^2}{a}}d}} \tag{15}$$

$$B(s) = \frac{T_w - T_0}{s} \times \frac{1}{1+e^{2\sqrt{\frac{s+\tau s^2}{a}}d}} \tag{16}$$

Substituting Equations (15) and (16) into Equation (11) gives the following:

$$\overline{T}^*(x,s) = \frac{T_w - T_0}{s} \times \frac{1}{1-e^{-2\sqrt{\frac{s+\tau s^2}{a}}d}} e^{-\sqrt{\frac{s+\tau s^2}{a}}x} + \frac{T_w - T_0}{s} \times \frac{1}{1-e^{2\sqrt{\frac{s+\tau s^2}{a}}d}} e^{\sqrt{\frac{s+\tau s^2}{a}}x} \tag{17}$$

Laplace transform is performed on Equation (17):

$$T^*(t) = \frac{\ln 2}{t}\sum_{i=1}^{N} C_i T^*\left(\frac{\ln 2}{t}i\right) \tag{18}$$

$$C_i = (-1)^{i+N} \times \sum_{k=int\left[\left(\frac{i+1}{2}\right)\right]}^{\min\left(i,\frac{N}{2}\right)} \frac{k^{\frac{N}{2}}(2k)!}{\left(\frac{N}{2}-k\right)!k!(k-1)!(i-k)!(2k-i)!} \tag{19}$$

Because $T^* = T - T_0, \therefore\ T = T^* + T_0$

Finally, the following is concluded:

$$T(t) = \frac{\ln 2}{t}\sum_{i=1}^{N} C_i T^*\left(\frac{\ln 2}{t}i\right) + T_0 \tag{20}$$

Equation (20) is a transient heat conduction model of coating tool cutting heat derived based on non-Fourier heat conduction.

III. EXPERIMENTAL SETUP

The cutting temperature of coated tools is measured using thermocouples in order to validate the analytical model. H13 hardened steel was chosen as the work piece material for the turning experiment. Figure 3a illustrates the experimental setup. Pictures of the experimental setup are shown in Figure 3b. The workpiece used in this experiment was a cylindrical bar with 300 mm length and 70 mm external diameter. The cutting speeds were vc = 35.9 m/min, 56.1 m/min, 89.2 m/min, 110.7 m/min, 197.8 m/min, and 244.4 m/min, respectively. The feed rate was f = 0.2 mm/rev, while the depth of cut was ap = 0.2 mm. The machining operation was then performed with a constant chip section and a constant cutting speed.

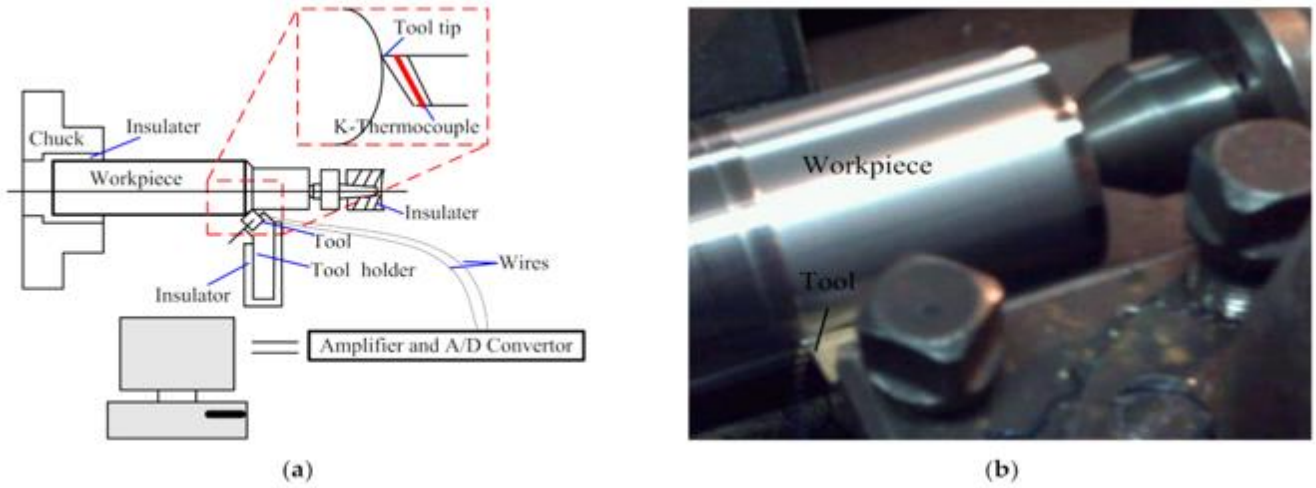

FIGURE 3: Tool temperature measurement set-up (a) schematic and (b) actual photograph.

A KC735M mono layer cutting tool coated with TiN layer of carbide substrate was used. The thickness of the coated layer is 2 µm, given by the manufacturer. A standard Scanning electron microscope at a fracture cross-section of the coated sample was given to the thickness measurements shown in Figure 4.

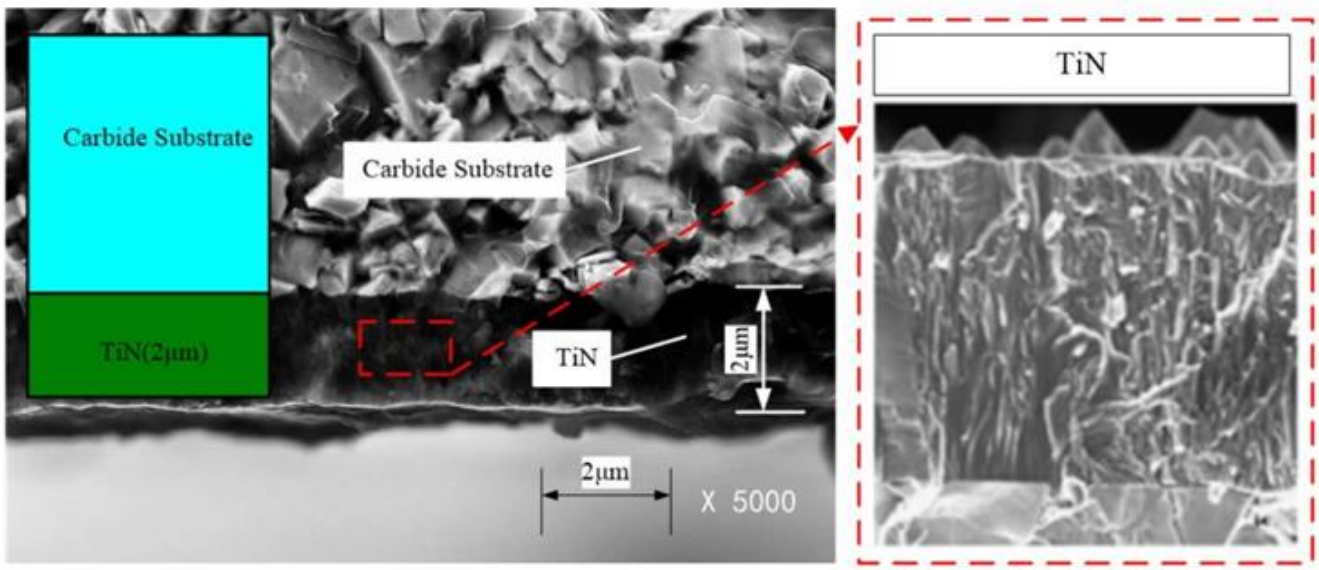

FIGURE 4: Structure of carbide substrate and components of KT315 coated cutting tool. Magnification: 5000×

Through the development of wireless temperature measurement, experimental work was done to gauge the cutting tool's temperature. The turning tool contains an incorporated thermocouple sensor. For the thermocouple's sensor installation, the tool bored two mounting holes. The distance between the tool tip and the mounting hole is 2 mm. The mounting hole is 1 mm in diameter and 1 mm in depth. To guard against damage from the cutting chips, the sensor's top was covered with high temperature structural adhesive, or HT-CPS. Temperature difference amplifies the electric voltage that is converted. Through the amplifier and A/D convertor, the electric signals can be converted from the sensor to the computer.

IV. RESULTS AND DISCUSSION

To ensure a high-quality product, diagrams and lettering MUST be either computer-drafted or drawn using India ink.

Figure captions appear below the figure, are flush left, and are in lower case letters. When referring to a figure in the body of the text, the abbreviation "Fig." is used. Figures should be numbered in the order they appear in the text.

Table captions appear centered above the table in upper and lower case letters. When referring to a table in the text, no abbreviation is used and "Table" is capitalized. According to the transient heat conduction model, the computing process is

programmed in MATLAB (Version 2017b, MathWorks Inc, Natick, MA, USA). The equivalent temperature of rake face is assumed to be $T_w = 300^0$C. The selected thickness of the coating is $d = 2$ μm. The physical properties of TiN coatings and H13 steel are shown in Table 1.

TABLE 1
PHYSICAL PROPERTIES OF TiN COATING AND H13 [1,20].

Material	Thermal Conductivity, λ (W/m·^{0}C)	Thermal Diffusivity, a (m^2/s)	Density, ρ (kg/m^3)	Young's Modulus, E (Gpa)
TiN coating	23	5.07×10^{-7}	4650	250
H13 steel	28.6	5.07×10^{-6}	7800	211

4.1 Experimental Verification

Figure 5 depicts the cutting temperature distribution as determined by the thermocouple data and the analytical model, respectively. The temperature that is estimated is that at the thermocouple measurement point, which is located 1 mm away from the rake face. Figure 5 shows a linear relationship between the calculated and measured temperatures; the function is y = x. The trends in the numbers that were determined through calculation and measurement are generally consistent and good. The predicted temperature of the thermocouple measurement point revealed a comparable trend to the measured temperature at the same measurement point, according to the transient analysis model. As seen in Figure 5b, the estimated and actual temperature profiles are plotted at various cutting speeds.

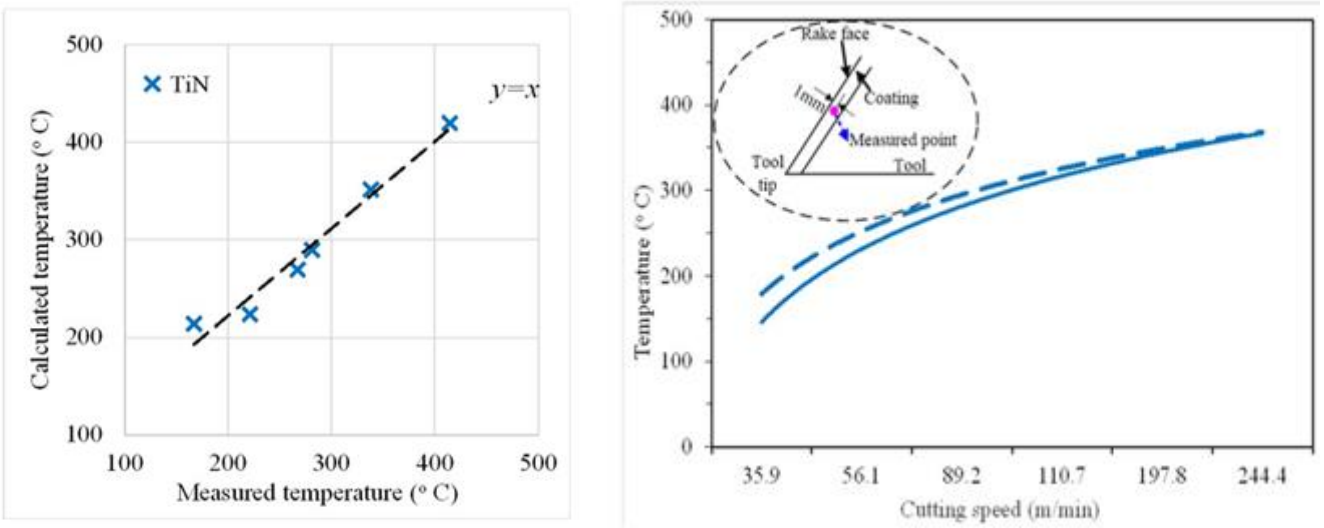

(a) **(b)**

FIGURE 5: The temperature distribution of TiN-coated tools: (a) relationship between measured and calculated values and (b) measured and calculated values versus cutting speed

In the modelling process, the analytical model is simplified and contained hypothesis conditions. The boundary is simply described as an adiabatic boundary or a thermostatic boundary when the convective heat conduction coefficient of the boundary is infinitesimal. During the actual cutting process, the coated tool and workpiece material's heat dissipation is neglected. The analytical model is effective since the expected error is less than 12%, which is an acceptable level for industrial applications.

4.2 Effects of Cutting Time on Temperature Distribution

The cutting temperatures of TiN-coated tools are computed using the transient heat conduction model, as shown in Figures 6 and 7. The temperature of the coating surface in Figure 6 rises from 200C to an assumed equivalent temperature of 3000C in 0.5 seconds (0.01m from the coating surface), while the temperature of the coating-substrate interface rises from 200C to nearly 2100C (2 m from the coating surface). Different temperature values are present simultaneously at various locations inside the

coating. The coating surface temperature (0.01 m from the coating surface) is higher than the coating body temperature (0.1 m from the coating surface) when the cutting time of 2 s is reached. The temperature drops as you get further away from the coated surface during the same cutting process. This suggests that the heat conduction during cutting has a finite velocity.

Investigations were done into how cutting times of 0.0001, 0.001, 0.01, 0.1, 1, 3, and 10s affected temperature distribution. As the distance from the coated surface rises, the difference in cutting temperature at various cutting periods exhibits a decreasing trend from 3000C (i.e., the boundary temperature). Figure 7 shows that when the cutting time increases, the difference values between the maximum temperature (i.e., the coating surface temperature) and the minimum temperature (i.e., the coating-substrate interface temperature) decrease. The fluctuations in cutting temperature over the course of cutting can be used to identify the heat conduction states. When the cutting time is 1 second, heat conduction with high intensity occurs. Transient heat conduction occurs when the cutting time is between 1 and 10 seconds, yet the thermal disturbance is not immediately apparent. When the cutting time is greater than 10 s, the temperature change is minimal and the transition from the transient state to the steady state is slow.

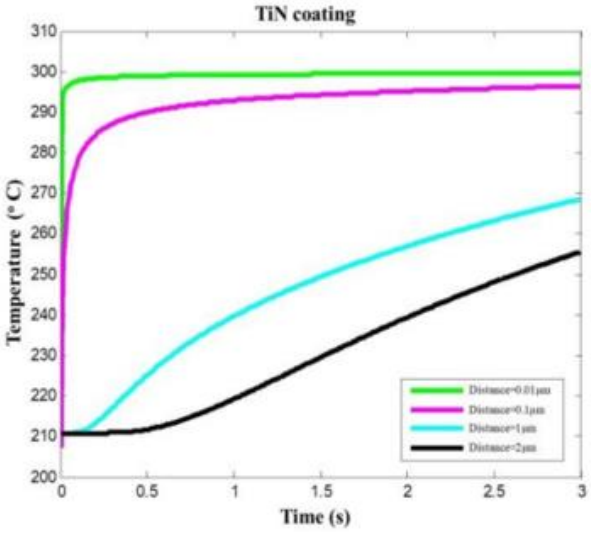

FIGURE 6. Temperature prediction at different locations within the TiN-coated tool coating

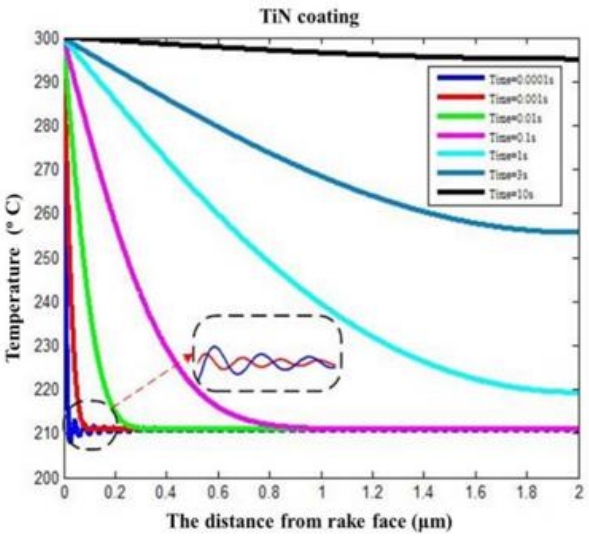

FIGURE 7. Temperature prediction in TiN coating changing over distance from coating surface

The temperature shows a rapid reduction and delays the change process in the heat conduction process within a very cutting short time, namely, in the unsteady-state heat conduction phase (i.e., blue and red curves in Figure 7). The temperature fields indicated by the blue and red curves were rapidly reduced to a certain temperature (210 ◦C) and presented a fluctuating change trend (the partial view as shown in Figure 7). The temperature fields sometimes are higher than the certain temperature, and sometimes are less than the certain temperature. The temperature calculation with transient heat conduction analytical model shows that the temperature changes are a delay rapid growth process. The fluctuation of the red curve is a not obvious owing to the decreased transient degree. The fluctuations of the subsequent curves disappear gradually, as the heat conduction states changes from the intensity transient-state to transient-state and then to steady-state as the cutting time increases.

4.3 Temperature Distribution with Fourier and Non-Fourier Heat Conduction

Figure 8 illustrates the stark contrast between the temperatures anticipated by Fourier and non-Fourier heat conduction at the same cutting time and same place. At intensities of transient heat conduction, the temperature determined by Fourier heat conduction does not exhibit a thermal disturbance. The process depicted begins with a decline at the 300 °C boundary temperature. Unsteady state heat conduction rapidly decreases as temperature increases when non-Fourier heat conduction is used to compute it. After then, there is a process of temperature fluctuation and change. The fluctuation changes progressively vanish and the temperature decreases with the reduction of the transient degree.

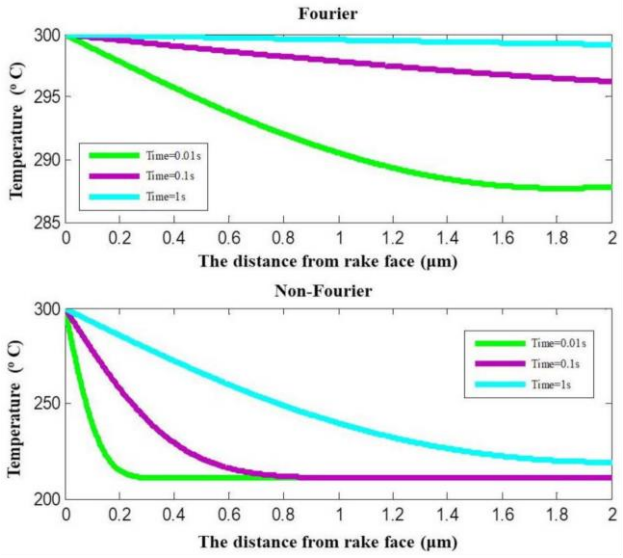

FIGURE 8: Temperature prediction with Fourier and non-Fourier heat conduction.

Figure 9 respectively displays the temperatures calculated using non-Fourier heat conduction and Fourier heat conduction at the coating surface and coating-substrate interface. The predictions by the two models for the temperature at the coating-substrate contact are considerably dissimilar. The calculated temperature difference between the two models at 0.01s cutting time is 77.10C. The predicted temperature difference between the two models when the cutting duration is 10 s is 4.90C. The temperature tends to stabilize when the cutting time is sufficient and heat conduction reaches its steady state. The cutting heat can be characterized as transient heat conduction with a finite velocity that travels through the thin film coating on the tool surface to the inside of the tool.

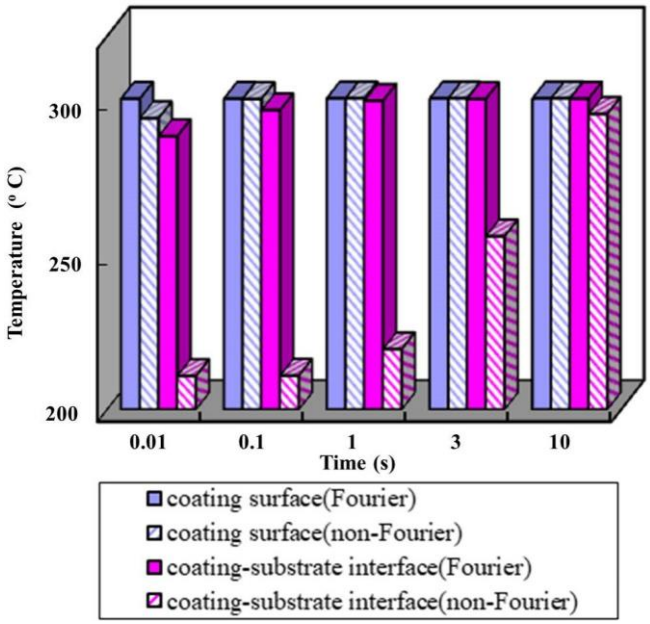

FIGURE 9: Temperatures prediction at coating surface and coating–substrate interface.

V. CONCLUSION

The cutting temperature of a monolayer coated tool in both steady-state and unsteady-state conditions was examined in this research. The cutting temperatures of TiN-coated tools under various heat conduction conditions were computed based on the analytical models. The following conclusions were drawn:

1. When the cutting duration was sufficiently small, the temperatures underwent a fluctuating change process, which progressively vanished as the transient degree weakened. The cutting temperature rose and eventually stabilized as the cutting time increased, shifting from a transient-state to a steady-state in terms of heat conduction. The lower the tool body temperature is, the closer it is to the coated surface while the cutting time is constant.

2. It is discovered that the cutting heat transient conduction of coated tool machining exhibits the non-Fourier heat conduction effect. The non-Fourier heat conduction model may effectively capture the thermal disturbance and thermal delay brought on by thermal shock when the heat conduction is transient heat conduction.

3. The prediction error is less than 12%, which is acceptable for industrial applications and proves the efficiency of the developed model.

REFERENCES

[1] Kalss, W.; Reiter, A.; Derflinger, V.; Gey, C.; Endrino, J.L. Modern coatings in high performance cutting applications. Int. J. Refract. Met. Hard Mater. 2006, 24, 399–404.

[2] Klocke, F.; Krieg, T.; Gerschwiler, K.; Fritsch, R.; Zinkann, V.; Pöhls, M.; Eisenblätter, G. Improved cutting processes with adapted coating systems. CIRP Ann. 1998, 47, 65–68.

[3] Sandvik, C. Modern Metal Cutting: A Practical Handbook; Sandvik Coromant: Sandviken, Sweden, 1994.

[4] Yan, S.; Zhu, D.; Zhuang, K.; Zhang, X.; Ding, H. Modelling and analysis of coated tool temperature variation in dry milling of Inconel 718 turbine blade considering flank wear effect. J. Mater. Process. Technol. 2014, 214, 2985–3001.

[5] Baïri, A.; Laraqi, N. Effect of thickness and physical properties of films on the thermal behavior of a moving rough interface. Eur. Phys. J. Appl. Phys. 2004, 26, 29–34.

[6] Benabid, F.; Benmoussa, H.; Arrouf, M. A thermal modelling to predict and control the cutting temperature. The simulation of face-milling process. Glob. J. Res. Eng. 2014, 74, 37–42.

[7] da Silva, M.B.; Wallbank, J. Cutting temperature: Prediction and measurement methods—A review. J. Mater. Process. Technol. 1999, 88, 195–202.

[8] Grzesik, W.; Bartoszuk, M.; Nieslony, P. Finite element modelling of temperature distribution in the cutting zone in turning processes with differently coated tools. J. Mater. Process. Technol. 2005, 164, 1204–1211.

[9] Mozafarifard, M.; Toghraie, D.; Sobhani, H. Numerical study of fast transient non-diffusive heat conduction in a porous medium composed of solid-glass spheres and air using fractional Cattaneo subdiffusion model. Int. Commun. Heat Mass Transf. 2021, 122, 105192.

[10] Zehnder, A.T.; Rosakis, A.J. On the temperature distribution at the vicinity of dynamically propagating cracks in 4340 steel. J. Mech. Phys. Solids 1991, 39, 385–415.

[11] Cattaneo, C. A form of heat-conduction equations which eliminates the paradox of instantaneous propagation. Comptes Rendus 1958, 247, 431–433.

[12] Vernotte, P. Les paradoxes de la theorie continue de I'equation de la chleur. Comptes Rendus 1958, 246, 3154–3155.

[13] Kiwan, S.; Al-Nimr, M.; Al-Sharo'a, M. Trial solution methods to solve the hyperbolic heat conduction equation. Int. Commun. Heat Mass Transf. 2000, 27, 865–876.

[14] Barletta, A.; Zanchini, E. Three-dimensional propagation of hyperbolic thermal waves in a solid bar with rectangular cross-section. Int. Commun. Heat Mass Transf. 1999, 42, 219–229.

[15] Schwarzwlder, M.C.; Myers, T.G.; Hennessy, M.G. The one-dimensional Stefan problem with non-Fourier heat conduction. Int. J. Therm. Sci. 2020, 150, 106210–106211.

[16] Ferreira, D.C.; dos Santos Magalhães, E.; Brito, R.F.; Silva, S.M.M. Numerical analysis of the influence of coatings on a cutting tool using COMSOL. Int. J. Adv. Manuf. Technol. 2018, 97, 1305–1314.

[17] Zhang, J.J.; Liu, Z.G. Transient and steady-state temperature distribution in monolayer-coated carbide cutting tool. Int. J. Adv. Manuf. Tech. 2017, 91, 59–67.

[18] Dogu, Y.; Aslan, E.; Camuscu, N. A numerical model to determine temperature distribution in orthogonal metal cutting. J. Mater. Process. Tech. 2006, 171, 1–9.

[19] Ma, L.W.; Cairney, J.M.; Hoffman, M.J.; Munroe, P.R. Effect of coating thickness on the deformation mechanisms in PVD TiN-coated steel. Surf. Coat. Technol. 2010, 204, 1764–1773.

[20] Grzesik, W.; Nieslony, P.; Grzesik, W. A computational approach to evaluate temperature and heat partition in machining with multilayer coated tools. Int. J. Mach. Tools Manuf. 2003, 43, 1311–1317.